A STRUCTURAL STUDY OF THE SELF-ASSOCIATION OF DIFFERENT STARCHES IN PRESENCE OF BACTERIAL CELLULOSE FIBRILS

P. Díaz-Calderón[1,2]*, E. Simone[3], A.I.I. Tyler[3], J. Enrione[1,2] and T. Foster[4,5]

[1]Biopolymer Research & Engineering Laboratory (BIOPREL), School of Nutrition and Dietetics, Faculty of Medicine, Universidad de los Andes, Chile. Av. Monseñor Alvaro del Portillo Nº12.455, Las Condes, Santiago, 7620001, Chile.

[2]Center for Biomedical Research and Innovation (CIIB), Faculty of Medicine, Universidad de los Andes, Chile. San Carlos de Apoquindo Nº2.200, Las Condes, Santiago, 7620001, Chile.

[3]Food Colloids and Bioprocessing Group, School of Food Science and Nutrition, University of Leeds, Leeds, LS2 9JT, United Kingdom.

[4]Campden BRI, Station Road, Chipping Campden, Gloucestershire, GL55 6LD, United Kingdom.

[5]Division of Food Sciences, Nutrition and Dietetics, The University of Nottingham, Sutton Bonington Campus, Loughborough, LE12 5RD, United Kingdom.

Corresponding author: P. Díaz-Calderón, pdiaz@uandes.cl

Abstract

A multi-analytical study was performed to analyse the effect of bacterial cellulose (BCF) on the self-association of starches with different amylose content (wheat, waxy-maize), assessing macrostructural properties (rheology, gel strength) and some nano and sub-nano level features (small and wide-angle X-ray scattering). Although pasting viscosities and G' were significantly increased by BCF in both starches, cellulose did not seem to promote the self-association of amylose in short-range retrogradation. A less elastic structure was reflected by a 2-3-fold increase in loss factor (G''/G') at the highest BCF concentration tested. This behavior agreed with the nano and sub-nano characterisation of the samples, which showed loss of starch lamellarity and incomplete full recovery of an ordered structure after storage at 4° C for 24h. The gel strength data could be explained by the contribution of BCF to the mechanical response of the sample. The information gained in this work is relevant for tuning the structure of tailored starch-cellulose composites.

Keywords: starch; bacterial cellulose; retrogradation; viscoelasticity; nanostructure; gel strength.

1. Introduction

Starch and cellulose are the most available biopolymers in nature. Both have been extensively used in the food industry due to them being the most important energy source for humans in the case of starch, and as a low-calorie ingredient and structuring material in the case of cellulose and its derivatives. However, during recent years starch, cellulose and their composites have been studied for some other high-value applications in different technological fields such as the development of edible films and thin coatings (Basiak, Lenart, & Debeaufort, 2017; Ilyas, Sapuan, Ishak & Zainudin, 2018; Li, Xie, Hasjim, Witt, Halley & Gilbert, 2015), design of novel composites and bio-plastics for packaging (Fazeli, Keley & Biazar, 2018; Hornung et al., 2018; Luchese, Spada & Tessaro, 2018) or in the design of polymer scaffolds for wound healing and tissue engineering (Sadashiv et al., 2018; Velasquez, Pavon-djavid, Chaunier, Meddahi-pellé & Lourdin, 2015), to name a few. Since cellulose has been found to act as a filler in composite materials, cellulose has been incorporated to starchy systems in order to enhance some of the poor physical properties described in starch-based composites such as brittleness, low mechanical strength, high gas permeability, a reduced water barrier and high hygroscopicity (Benito-González, López-Rubio & Martínez-Sanz, 2019; Ilyas et al., 2018).

However, the rational design of advanced materials based on starch-cellulose composites is based on the tailored manufacture of self-associated and self-assembled polysaccharides (Valencia et al., 2019). Thus, the development of starch-cellulose composites requires a deep understanding of the structural features of these composites, and how some of their physical properties are defined by the self-association of starch polymers (amylose and amylopectin), and what is the effect of cellulose on such self-association. In the case of starch-based composites, the current literature focused on relating the structural and physical changes with the well-known phenomenon of gelatinisation and retrogradation, and their corresponding granular disruption and molecular self-association mechanism, respectively. For instance Benito-González et al. (2019) reported a significant enhancement of the mechanical and water barrier performance of corn starch films in the presence of cellulose fillers (from waste biomass), which is explained by

79 a combination of incomplete gelatinisation allowed by reduced moisture content and a limited
80 degree of retrogradation (self-association) caused by cellulose. Zhang et al. (2018a) tested the
81 effect of pectin with different molecular weights on gelatinisation and retrogradation of corn
82 starch, concluding that high molecular weight pectin hindered the gelatinisation and restricted
83 the swelling of starch granules, which significantly reduced the relative crystallinity of starch in
84 mixture with pectin during storage. Complementary to this, Qiu et al. (2014) suggested that
85 reducing amylose leaching during gelatinisation of corn starch by inclusion of corn fiber gum (an
86 arabinoxylan constituent of hemicellulose B) could be responsible for the decrease in starch
87 retrogradation during the cooling stage, which was well-reflected by the lowering of the final
88 viscosity assessed by Rapid Visco Analysis (RVA).
89 Similarly, over recent years the interest in exploring alternative sources of cellulose has
90 increased. In addition to plant sources, cellulose can also be produced by several Gram-negative
91 bacterial strains, with *Gluconacetobacter xylinus* being the most efficient producer of cellulose
92 (Ullah, Santos & Khan, 2016). These microorganisms are able to create in their extracellular
93 matrix a complex network of cellulose fibrils, each made up of (1→4) β-glycosidic linked glucose
94 units, which form highly regular intra- and inter molecular hydrogen bonds resulting in a weak
95 gel structure of cellulose fibrils (Shi, Zhang, Phillips & Yang, 2014). In terms of molecular
96 structure and size, bacterial cellulose is predominantly left-hand twisted, with individual
97 nanofibrils having cross-sectional dimensions in the nanometer range, with an estimated
98 thickness of 3-8 nm and several microns in length, which can then aggregate to form microfibrils
99 with 25-100 nm in width (Lee, Buldum, Mantalaris & Bismarck, 2014; Shi et al., 2014). Bacterial
100 cellulose is characterized by its high purity (free of components such as lignin and hemicellulose),
101 high crystallinity and higher surface area than the cellulose obtained from plant sources, which
102 would explain its exceptional mechanical properties and stability. Along with the mechanical
103 stability, bacterial cellulose fibrillar composites have high-water absorption capacity in the wet
104 state, showing hydrophilicity, flexibility and full *in vivo* biocompatibility, making this material

105 feasible to be used in a wide variety of applications in healthcare, artificial skin, *in vivo* implants,
106 artificial blood vessels and wound healing scaffolds (Chang & Chen, 2016; Fadel et al., 2017;
107 Rajwade, Paknikar & Kumbhar, 2015; Ullah et al., 2016; Yang et al., 2014; Zang et al., 2015). In
108 addition, bacterial cellulose has been extensively used as a reinforcement material for polymeric
109 networks, which explains its utilisation in packaging technology, which is also supported by its
110 biodegradability (He et al., 2009; Miao & Hamad, 2013; Müller, Laurindo & Yamashita, 2009; Shah,
111 Ul-Islam, Khattak & Park, 2013). The use of bacterial cellulose as a multifunctional food
112 ingredient to control the properties of food and beverages as a thickener, stabiliser and texture
113 modifier has also been investigated (Paximada, Tsouko, Kopsahelis, Koutinas & Madala, 2016;
114 Shi et al., 2014; Ullah et al., 2016).
115 Interestingly, information on the role of bacterial cellulose fibrils (BCF) in the tailored design of
116 starch-cellulose composites, and more specifically the effect of BCF on the self-association of
117 the starch polymers (amylose and amylopectin) is scant. A recent study carried out by Díaz-
118 Calderón, MacNaughtan, Hill, Foster, Enrione & MItchell (2018) reported how the gelatinisation
119 of starch from different sources (wheat, maize and waxy-maize) was modified by the addition of
120 BCF. This work showed a marked change in pasting properties specially in both final viscosity
121 and setback viscosity, which were significantly increased by the addition of BCF in a
122 concentration range between 0.5-10% (w/w). The literature has explained the significant
123 increase in both setback and final viscosity in starchy systems during the cooling stage in RVA
124 testing, by the tendency of the amylose present in the hot paste to self-associate upon the
125 decrease in temperature (Balet et al., 2019; Belitz et al., 2009; BeMiller & Huber, 2008). However,
126 the literature lacks studies reporting the effect of BCF on the self-association of starch polymers
127 at both the macroscale and nanostructural level. What is currently missing is a detailed study on
128 how cellulose from alternative sources (such as bacterial cellulose) modifies the self-association
129 of starch polymers. Such knowledge can be used for the design of novel, sustainable materials
130 with tunable physical properties (e.g. transport, mechanical, optical among others). In fact,

131 starch-bacterial cellulose composites can find numerous used in applications for bioengineering
132 as well as in the pharmaceutical and food industry.
133 In this work we focused on the study of self-association in starch-BCF mixtures, through multi-
134 analytical testing oriented to evaluate structural changes taking place at a macrostructural scale
135 (viscosity, viscoelasticity and gel strength) and at nano and sub-nano structural scale (lamellar
136 structure of starch by SAXS and crystallographic structure by WAXS). Possible differences
137 attributed to the amylose content among starch samples were also included as a part of this
138 study to test the hypothesis that cellulose, in some way, promotes self-association of amylose.
139

140 **2. Materials and Methods**

141 2.1. Materials

142 Native wheat starch (~25-29% amylose) and native waxy maize starch (essentially pure
143 amylopectin, containing only trace amounts of amylose) were purchased from Sigma Aldrich
144 (Germany) in powder form. Dried sheets of bacterial cellulose were kindly provided by Vuelo
145 Pharma (Brazil). Starch and bacterial cellulose were used as received without further purification
146 and stored at room temperature until further use.
147

148 2.2. Preparation of hydrated paste of BCF

149 Hydrated paste of BCF was prepared to be blended with native starch to have starch suspension
150 with BCF concentration of 0, 0.5, 2, 6 and 10% w/weight dry cellulose (Equation 1). For this
151 purpose, well-defined amounts of bacterial cellulose dried sheets were weighed and processed
152 prior to mixing, following the protocol reported by Quero et al. (2015). Briefly, weighed amounts
153 of cellulose were held overnight in excess of distilled water in order to promote full hydration.
154 Then, the bacterial cellulose in excess of water was homogenized using a high-power kitchen
155 blender (Osterizer, USA. 300 W) for 20 min, and vacuum filtered by using 8 mm diameter filter
156 paper (Whatman 541, USA). Finally, the filtered BCF was used to obtain hydrated paste with well-

157 defined concentration (0-10% w /weight) and stirred for 15 min at room temperature (20 ± 2° C)
158 to provide homogeneous paste. Figure SF-1 (Supplementary file) shows how the visual
159 appearance of hydrated paste of BCF.
160
161 $$BCF\ Concentration\ \left(\%, \frac{w}{w}\right) = \left(\frac{BCF\ weight}{BCF\ weight + Starch\ Weight}\right) x100$$ Equation 1
162
163 2.3. Pasting properties during cooling stage by Rapid-Visco-Analysis in starch-BCF blends
164 Pasting properties of starch-BCF blends were assessed by Rapid-Visco-Analysis (RVA 4500,
165 Perten Instruments, Australia) in accordance with the methodology proposed by Sullo and Foster
166 (2010) with minor modifications. 2 g of native starch was weighed in aluminum canisters and 25
167 mL of hydrated paste of BCF with different cellulose concentrations (Section 2.2.) were
168 transferred using a micropipette. The canister was then inserted into the instrument and pasting
169 profiles were obtained as a function of temperature: holding at 25°C during 2 min, heating
170 between 25 and 95°C at 13.5°C/min, holding at 95°C for 5 min, cooling to 25 °C at 13.5°C/min
171 and holding at 25°C for 5 min. The analysis was performed under constant stirring (160 rpm). As
172 the goal of this work was focused to understand the self-association of starch after the complete
173 gelatinisation of native granules, the pasting parameters evaluated were hold viscosity (minimum
174 paste viscosity achieved after holding at the maximum temperature) and final viscosity (viscosity
175 at the end of the RVA test). Hence, only final viscosity and setback viscosity (difference between
176 final viscosity and hold viscosity) were further discussed. All measurements were carried out at
177 least in triplicate.
178
179
180
181 2.4. Viscoelasticity of starch-BCF blends by rheology

182 The changes in viscoelasticity of starch-BCF blends were carried out by rheology (Discovery HR-
183 2, TA Instrument, USA). Once the RVA test was completed, the RVA canister was held for 5 min
184 at ambient temperature and then a sample was collected from the canister and transferred to
185 the rheometer. A flat plate geometry (5 cm diameter) was used for analysis and a 300 μm gap
186 was selected for testing. Changes in storage modulus (G', Pa) and loss modulus (G'', Pa) were
187 obtained through a frequency sweep carried out to analyse the behavior of G', G'' and loss factor
188 (G''/G') as a function of angular frequency from 0.01 to 648 rad/s, at 0.05% strain which was
189 within the linear viscoelastic range (LVR) previously defined by a small deformation test (0.01-
190 100%) at 25°C. The analysis considered at least five replicates per experimental condition.
191
192 2.5. Small and Wide Angle X-ray Scattering (SAXS-WAXS) of starch-BCF blends
193 For these analysis samples processed by RVA were also used. After the RVA testing was finished,
194 the samples were stored at 4 ± 1°C for 24 ± 2 h. The samples were then snap frozen by immersion
195 in liquid nitrogen and immediately freeze dried. Once the samples were completely dried, they
196 were ground using a small mortar and stored at -20°C until further use. Samples prepared by this
197 protocol were used for analysis by small and wide-angle X-ray scattering (SAXS and WAXS,
198 respectively).
199 X-ray experiments on freeze dried solid powders of starch-BCF samples were carried out at
200 Diamond Light Source (DLS, Didcot, UK) on beamline I22. The synchrotron X-ray beam was tuned
201 to a wavelength of 0.069 nm. The distance between the sample and detector was set at 8.7 m
202 and the 2D powder diffraction patterns were recorded on a Pilatus 2M (Dectris Ltd) and Pilatus
203 P3-2M-DLS-L (Silicon hybrid pixel detector, Dectris Ltd) detectors for the SAXS and WAXS
204 patterns, respectively. Samples were inserted in 2 mm diameter glass capillaries and measured
205 at ambient temperature. Diffraction images were analysed using the DAWN software (Filik et
206 al., 2017). The obtained two-dimensional SAXS and WAXS patterns were radially integrated to
207 give one-dimensional scattering intensity profiles. For the WAXS data, a background correction

208 was performed by subtracting the minimum value for each measurement to all the points of the
209 pattern (in this way all samples have their minimum value at zero).
210 Pure bacterial cellulose, freeze dried mixtures of native starch-BCF samples and freeze-dried
211 gelatinised mixtures of starch and BCF were instead characterized using an X-ray scattering
212 camera setup (SAXSpace, Anton Paar, Austria) that uses a line-shaped beam of Cu Kα radiation
213 with a wavelength λ = 0.154 nm. Dried BCF sheets and fibrillar samples were inserted into a
214 vacuum-tight paste cell and measured at 25° C (exposure time of 30 min). Gelatinised samples
215 were measured using the same conditions. A Mythen X-Ray detector system (Dectris Ltd., Baden,
216 Switzerland) was used to record the 1D scattering patterns and the SAXStreat and SAXSQuant
217 software (Anton Paar, Graz, Austria) were used to pre and post process the data. Origin 2019b
218 was used to analyse all X-ray scattering data.
219
220 2.6. Scanning Electron Microscopy (SEM)
221 Starch and BCF blends previously analysed by RVA testing, stored at 4 ± 1ºC for 24 ± 2ºC h and
222 freeze-dried were imaged using a Carl Zeiss EVO MA15 scanning electron microscope at
223 magnifications from 250X to 10.000X. Freeze dried and powered blends of starch and BCF were
224 arranged on Leit tabs attached to SEM specimen stubs and a 20 nm thick iridium coating was
225 applied before measurement.
226
227 2.7. Gel strength in retrograded starch-BCF blends
228 Measurements of gel strength were carried out on starch-BCF blends obtained after the
229 complete gelatinisation of starch. For these experiments, 400 mL of hydrated paste of BCF
230 prepared following the protocol previously explained (Section 2.2.) were prepared and 32 g of
231 native starch were added to each hydrated paste of BCF. Thus, starch suspension with BCF
232 concentration of 0, 0.5, 2, 6 and 10% w/weight dry cellulose were obtained. The blend was heated
233 to 90ºC and held at that temperature for 30 min, using a hot plate under mechanical constant

234 stirring (~160 rpm). Then, the complete gelatinised starch-BCF blend was transferred to
235 aluminum pans (5 cm height, 7 cm diameter), which were stored at 4 ± 1°C during 24 ± 2°C hours.
236 Each pan was covered by aluminum foil to avoid the loss of moisture during the storage. The gel
237 strength was measured using a texture analyser TA.XTplus (Stable Micro Systems, UK) with a
238 load cell of 5 kg and equipped with a 25 mm cylinder aluminum probe (P/25). Gel strength was
239 determined as the maximum force when the probe penetrated a distance of 4 mm into the starch-
240 BCF gels at 1 mm/s. The measurement was performed three times with five replications for each
241 starch-BCF gel.
242
243 2.8. Statistical analysis
244 Where appropriate, the statistical significance was assessed by a paired t-test (same variances)
245 and ANOVA using the Solver tool in Excel (Office 2016, Microsoft Corp.).
246
247 **3. Results and Discussion**
248 3.1. Pasting properties during cooling stage in RVA in starch-BCF blends
249 In order to evaluate the effect of BCF on the self-association of starch during cooling, the final
250 viscosity and setback viscosity assessed during the controlled cooling stage by RVA testing are
251 shown in Table I (the whole RVA profile for wheat-BCF and waxy maize-BCF samples and pasting
252 properties are shown in Figure SF-2 and Table SF-1, respectively, Supplementary File). For both
253 wheat and waxy-maize starch, the presence of BCF produced a significant increase ($p < 0.05$) in
254 both final viscosity and setback viscosity. The literature has explained the increase in final and
255 setback viscosity during the cooling stage on RVA testing, with the tendency of the amylose and
256 amylopectin present in the starchy paste to retrograde, where chains realign themselves to form
257 a more ordered structure with the decrease in temperature (Balet et al., 2019; Belitz et al., 2009;
258 BeMiller & Huber, 2008; Juhász & Salgó, 2008; Yildiz et al., 2013). However, the retrogradation is
259 a complex process that starts with the self-association of amylose in double-helical structures

during early stages followed by the re-association of branched polymers (amylopectin) after longer times of storage (Cui et al., 2018; Wang, Copeland, Niu & Wang, 2015). Hence, considering the time frame of the cooling stage on RVA, the increase in viscosity upon cooling could be explained by the formation of helical structures formed by amylose strands with only partial reassociation of amylopectin, which in the literature has been related with a short-range retrogradation (Cui et al., 2018; Wang, Copeland, Niu & Wang, 2015).

Our results showed that BCF produced higher values of setback viscosity in starch samples, which would suggest a higher capacity of starch polymers to reassociate. On the other hand, significant differences were observed in both final and setback viscosity values among all starch-BCF samples. Thus, all wheat starch samples showed significant higher values ($p < 0.05$) of final viscosity and setback viscosity compared to values obtained in waxy-maize starch at the same BCF concentration. This behavior highlights the contribution of amylose to the viscosity of starchy paste and could be explained by the capacity of amylose to self-associate during the final cooling stage of RVA testing. Likewise, the relative increase in viscosity during the cooling stage showed to be higher in wheat starch samples compared to the ratio obtained in waxy maize starch at the same BCF concentration. However, in wheat starch samples the increase in BCF concentration produced a diminishing in values of relative increase in viscosity (from 3.3 to 2.1, Table I), even approaching to those values of relative increase assessed in waxy-maize starch samples. Interestingly, our results showed than addition of 10%BCF produced an increase ~2X in setback viscosity of wheat starch (versus the control sample), whereas in waxy-maize starch the increase in setback viscosity was ~5X. Therefore, these contradictory results would not support the hypothesis that the presence of BCF promote the self-association of amylose. Moreover, previous studies have reported how complex is the BCF structure which does not allow a homogeneous distribution in the bulk when it is blended with starch or with gelatin (Díaz-Calderón et al., 2018; Quero et al., 2015). In that sense, the protocol to produce fibrils of bacterial cellulose is a crucial step to ensure a homogeneous mixing with starch; in particular the amount of energy supplied to

286 the cellulose to obtain individual fibrils into the bulk suspension or into the hydrated paste of
287 bacterial cellulose is a critical parameter to control.
288
289 **Table I:** Pasting properties (Final Viscosity and Setback Viscosity) assessed by RVA in starch-
290 bacterial cellulose fibrils (BCF) blends. Values in brackets correspond to standard deviation.
291 Different upper letters in the same column represent significant differences (p-value < 0.05).
292 The relative increase was defined as the ratio of final viscosity over hold viscosity in starch
293 samples containing the same amount of BCF.

	Final Viscosity (cP)		Setback Viscosity (cP)		Relative Increase	
BCF (%, db)	Wheat	Waxy-maize	Wheat	Waxy-maize	Wheat	Waxy-maize
0	1710.3 (45.5)^{a}	589.7 (4.7)^{a}	1193.0 (43.9)^{a}	308.6 (3.7)^{a}	3.3	2.1
0.5	1891.5 (30.3)^{b}	716.3 (5.1)^{b}	1272.5 (31.6)^{b}	374.0 (3.5)^{b}	3.1	2.1
2	2310.0 (18.9)^{c}	1015.3 (6.4)^{c}	1403. 3 (17.0)^{c}	498.7 (5.1)^{c}	2.5	2.0
6	3827.5 (124.9)^{d}	1951.3 (28.9)^{d}	2130.8 (73.6)^{d}	978.0 (62.1)^{d}	2.3	2.0
10	4689.3 (98.6)^{e}	2819.3 (17.0)^{e}	2425.5 (48.5)^{e}	1475.3 (108.1)^{e}	2.1	2.1

294
295
296 Therefore, the next sections of this work were focused on the analysis of the viscoelasticity, nano
297 and sub-nano characterisation of BCF-starch composites and gel strength testing, in order to
298 elucidate the effect of BCF on the re-association of starch occurring at least during early stages
299 of the retrogradation.
300
301 3.2. Viscoelasticity of starch-BCF blends
302 Viscoelastic characterisation of wheat and waxy-maize starch in blend with BCF were studied in
303 samples previously tested by RVA. The amplitude sweep carried out in both starch-BCF systems
304 helped to define the viscoelastic linear range (VLR), along with giving information about the
305 structural stability (Mezger, 2019) of starch-BCF blends (Figure 1). In wheat starch, a significant
306 increase in G' only in the samples containing BCF in concentration of 10% (w/w) was observed.

However, G' was slightly lower in samples containing BCF at 0.5% and 2%. The structural stability of wheat starch blends was slightly modified by BCF, as the critical strain at which the drop of G' took place was slightly decreased by BCF. The critical strain was observed around a value of oscillation strain of 50-70% (Figure 1). On the other hand, in waxy-maize starch, the presence of BCF increased the value of G' in samples with BCF concentration of 2% (w/w) or higher (Figure 1), and BCF did not affect the structural stability upon deformation. The critical strain was around 30% in all waxy-maize blends. These results suggest that BCF does not affect the structural stability of partly retrograded starch gels produced by starches with different amylose contents. Recently Chen, Fang, Federici, Campanella & Griffith Jones (2020) have explained the strengthening effect (increase in G') of potato starch gels and decreasing critical strain by the addition of protein fibrils being tested by amplitude sweep, caused by the aggregation and network formation of fibrils taking place at higher concentration of protein fibrils.

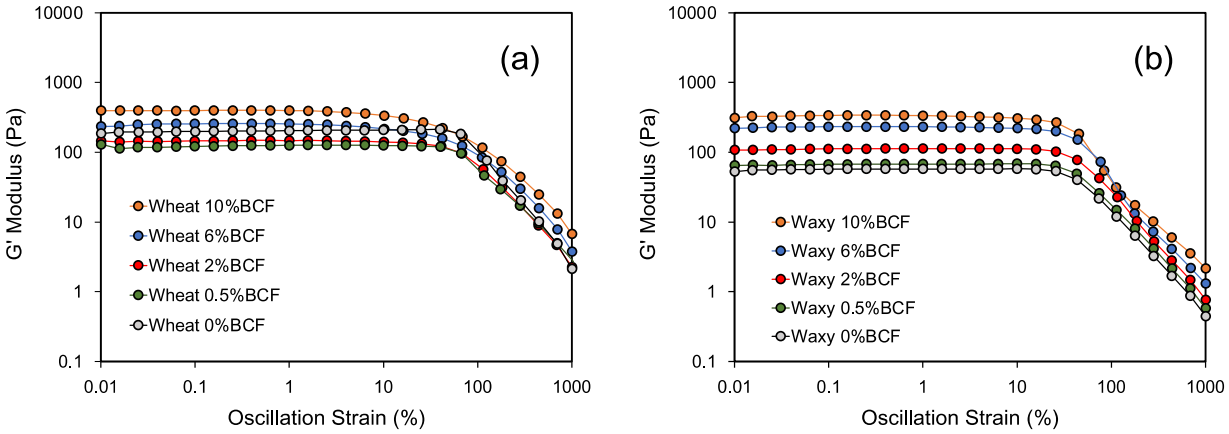

Figure 1. Amplitude sweep for starch-bacterial cellulose fibrils (BCF) blends tested at 25°C: (a) wheat starch, (b) waxy-maize starch

The results obtained from the frequency sweep test carried out on starch-BCF blends are presented in Figure 2. Following a similar trend previously observed in the amplitude sweep test, partly retrograded wheat starch blends (Figure 2a) showed a complex behavior whereby BCF at concentration of 0.5% significantly reduced the G' (p-value < 0.05), whereas an increase in G' was only observed in samples with BCF concentrations of 6% and 10% (w/w). All wheat-BCF blends showed a slight positive slope with respect to the angular frequency tested, and all blends tested showed G' > G'' in the whole frequency range demonstrating a gel-like behavior. As for the waxy-maize starch (Figure 2c), BCF produced a significant increase in G' (p-value < 0.05) proportional to the increase of BCF concentration in a similar way to what was previously observed in RVA testing regarding with final and setback viscosities. Following the same trend

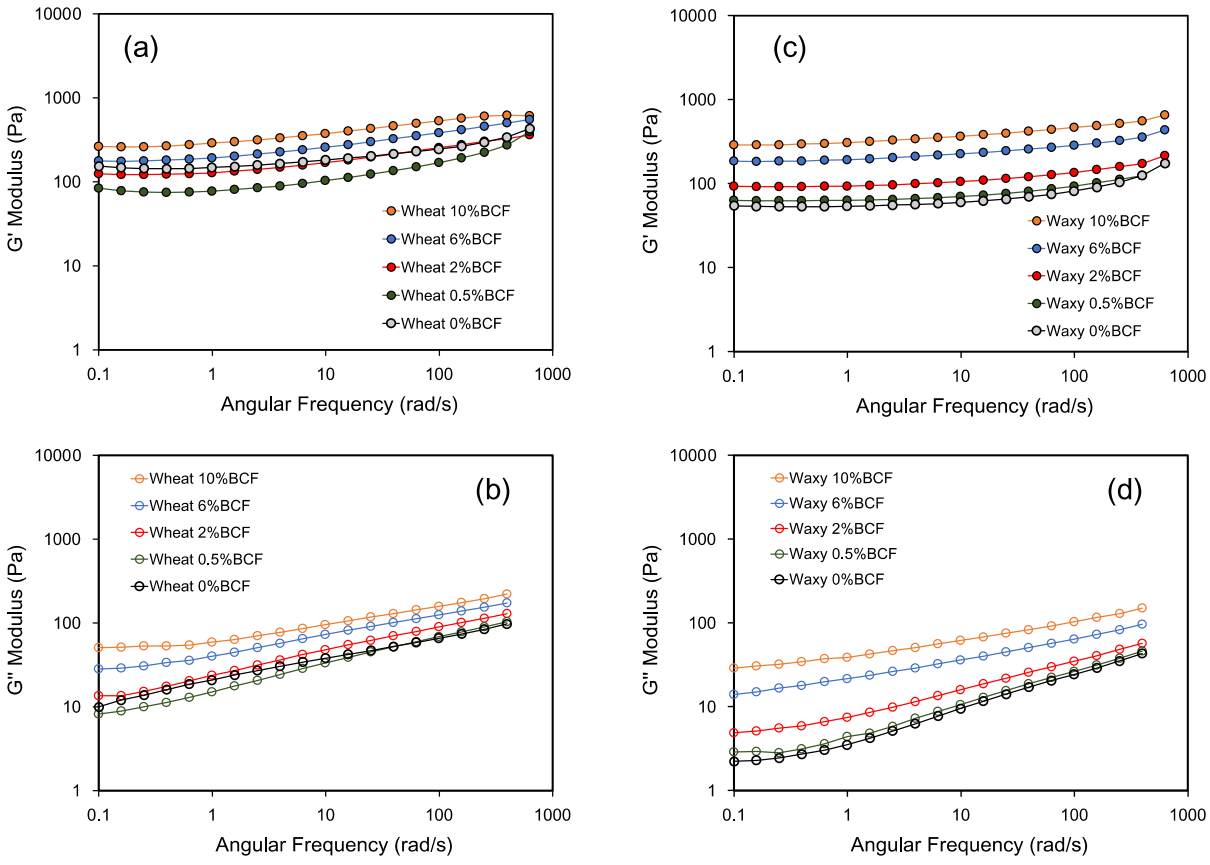

Figure 2. Frequency sweep in starch-bacterial cellulose fibrils (BCF) blends at 25°C: (a, b) wheat starch, (c, d) waxy-maize starch

observed in wheat starch blends, all samples also showed a slight positive slope in respect to the angular frequency tested, as well as gel-like behavior (G' > G''). Wheat-BCF blends with BCF concentration of 0% and 0.5% showed higher values of G' than waxy-BCF blends, which could be related to differences in amylose content. Interestingly, at BCF concentration of 2% and higher, there were not significant differences (p-value > 0.05) in G' between wheat and waxy-maize blends containing the same BCF concentration, as also observed in the amplitude sweep data (Figure 1). Further details about G' values are presented in Table SF-2 (Supplementary File).

In agreement with the increase of final viscosity and setback viscosity previously shown by RVA, partly retrograded starch blends containing higher concentrations of BCF were stiffer than the control sample, suggesting that the mechanism of self-association of starch is altered by the presence of BCF. However, changes in the loss factor (G''/G') as a function of BCF concentration should also be considered. Figure 3 shows the behaviour of the loss factor parameter for both starch-BCF blends. The trend of both control samples (0%BCF) is basically the same: a loss factor with values higher than 0.1 at high angular frequency and decreasing to values lower than 0.1 as the angular frequency is decreased. A loss factor value of 0.1 has been defined as the critical value to define a gel-like system as a "weak gel" in terms of viscoelasticity (Ikeda & Nishinari, 2001).

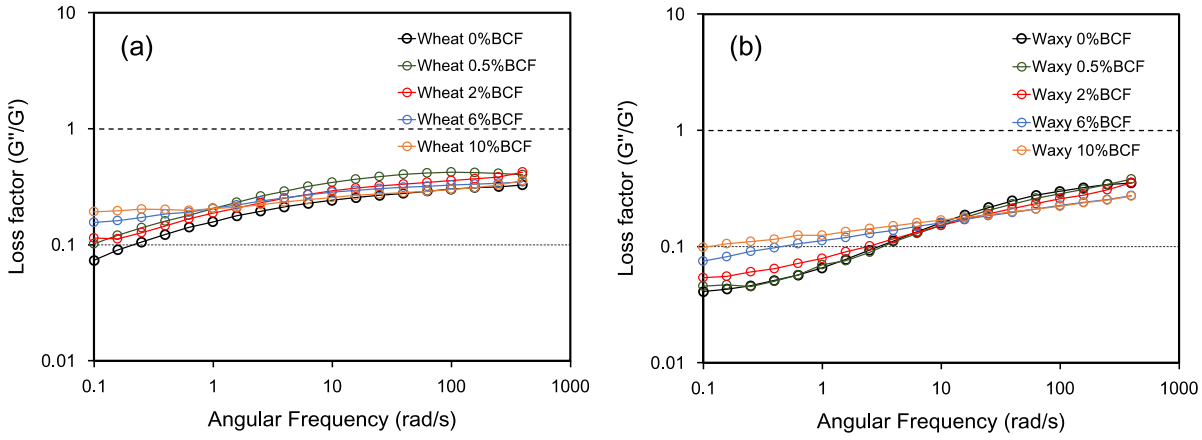

Figure 3. Loss factor (G''/G') of frequency sweep in starch-bacterial cellulose fibrils (BCF) blends at 25°C: (a) wheat starch, (b) waxy-maize starch

Therefore, this result shows the time-dependent characteristic of the starch retrogradation, by which the starch structure is becoming stiffer over time because of the self-association of the starch polymers during the retrogradation process.

Interestingly, from Figure 3 it is clear that BCF produced a significant increase in loss factor at lower values of angular frequency, and the effect was proportional to BCF concentration. In wheat starch, this behaviour was observed across all the angular frequency range tested (e.g. 0.5%BCF sample), but being more evident at lower values of frequency (< 1 rad/s). In waxy-maize this effect was more clearly observed at angular frequency values lower than 10 rad/s, although 6%BCF and 10%BCF decreased the loss factor at high angular frequency values. Since this effect was observed mainly at lower values of angular frequency it might suggest that viscoelastic behaviour would be characterised by a progressively less elastic system during the storage. In the literature, a decrease in loss factor has been correlated with a reduction of the amorphous fraction present in a starch based system explained by possible molecular reordering and re-crystallisation (Lionetto, Maffezzoli, Ottenhof, Farhat & Mitchell, 2005; Romdhane, Price, Miller, Benson & Wang, 2001). Thus, our results suggest that the starch-BCF blends do not regain an organized structure, with amylose and amylopectin only partly self-associated. Additionally, the viscoelastic behavior showed by our starch-BCF blends could be governed by the aggregation of cellulose fibrils taking place at higher concentration as has been suggested by Chen et al. (2020), which produced a weaker or less elastic structure compared to pure starch sample. Indeed, the condition of weak gel has been previously observed for pure bacterial cellulose gel systems (Díaz-Calderón et al., 2018). This fact could be also supported by how the bacterial cellulose was prepared before blending with starch. Presumably, the protocol used in this study did not allow a complete fibrillation of the cellulose, with complex cellulose aggregates forming, rather than individual fibrils. Complementary, Díaz-Calderón et al. (2018) showed a strong effect of BCF on starch paste viscosity arguing that the modulus-viscosity correlation could be explained by the volume fraction occupied by BCF and the structural domains of starch-cellulose in the blend. As

377 the volume occupied by BCF increases with concentration, this would provoke an increase in
378 concentration of starch in its own domain, and therefore the increase in concentration in both
379 domains would increase the overall modulus and the viscosity (Díaz-Calderón et al., 2018). On
380 the other hand, the effect of self-association of amylose would slow the effect of phase
381 rearrangement and dominance of the cellulose phase. Therefore, these results also suggest that
382 the self-association of amylose significantly affects the effectiveness of the cellulose fibrils to
383 begin to dominate the composite structure and subsequent rheological properties. For the waxy-
384 maize starch, which is essentially devoid of amylose, the gelatinisation of the granule allows the
385 cellulose 'phase' to create effective structures within the composite, but the leaching of amylose
386 from the wheat starch granules, and their subsequent self-association delay the effectiveness of
387 the BCF until much higher levels of BCF inclusion. That could be the reason why loss factor
388 observed in waxy-maize-BCF blends are lower than those observed in wheat-BCF at angular
389 frequency < 10 rad/s (Figure 2).
390 The effect of different hydrocolloids on viscoelastic properties of retrograded starches has been
391 extensively studied in the literature. For instance, Kim & Bemiller (2012) studied the effect of
392 some hydrocolloids such as xanthan, alginate, carrageenan, guar gum and modified cellulose
393 (methylcellulose, carboxymethylcellulose and hydroxypropylmethylcellulose) on the
394 viscoelasticity of retrograded pea starch, reporting a significant increase in loss factor ($\tan \delta$) in
395 all starch-hydrocolloid composites, which suggest a less structured system probably due to
396 interactions between amylose and hydrocolloids that inhibit network formation by amylose
397 molecules. Similar findings were reported by Leite et al. (2012) whom reported higher values of
398 G' in cassava starch by the addition of sodium carboxymethyl cellulose at low concentrations (up
399 to 0.45% w/v), but with corresponding higher values of loss factor reflecting a weaker and less
400 gel-like structure compared to pure starch. Complementary, Sun, Sheng, Xu, Chen & Chen (2016)
401 found that hydroxypropylmethylcellulose produced a small increase in G' and G'' of retrograded
402 rice starch but resulting in higher loss factor, despite the opposite effect being observed when

403 carboxymethylcellulose was added to rice starch. Most recently Ma, Zhu, Wang, Wang & Wang
404 (2019) reported that konjac glucomannan also weakened the structure of corn starch during
405 retrogradation which was correlated with the molecular weight of konjac glucomannan and
406 explained by possibly phase separation behaviour and polysaccharide interactions.
407
408 3.3. Small and Wide Angle X-Ray Scattering (SAXS/WAXS) of starch-BCF blends
409 The structure of freeze-dried samples of starch-BCF blends previously obtained by RVA and
410 stored at 4°C for 24 h were studied using X-ray scattering. Small angle X-ray scattering (SAXS)
411 patterns of native wheat, native waxy-maize starch and BCF are shown in Figure SF-3
412 (Supplementary File). Figure 4 (a and b) shows the SAXS patterns of native starch-BCF blends
413 before being processed by RVA. In both types of native starch, a peak was visible at around
414 $q=0.073$ $Å^{-1}$, which corresponds to the lamellar arrangement of semi-crystalline layers (growth
415 rings) in native starch granules (Doutch & Gilbert, 2013). The lamellar peak was still visible for a
416 BCF concentration of 0.5% w/w in the wheat starch blend and for concentrations up to 6% w/w
417 BCF for the waxy-maize starch samples. At high concentrations of BCF, a broad featureless peak
418 associated to this polymer ($q > 0.15$ $Å^{-1}$, clearly visible for pure BCF in the SAXS region as shown
419 in Figure SF-3, Supplementary File), overlaps with the lamellar peak of both waxy and wheat
420 starch. SAXS patterns of freeze-dried starch-BCF samples processed by RVA and stored at 4°C
421 for 24 hours did not present the characteristic starch lamellar peak at $q=0.073$ $Å^{-1}$ (Figure 4, c
422 and d), which confirms that the lamellar arrangement of starch was lost after the complete
423 gelatinization and hence there is loss of long range order. Interestingly, any other semi-crystalline
424 structure of starch was not recovered or developed during the storage time, and therefore the
425 starch-BCF blends were mainly amorphous. This behavior was observed for both starches and
426 at all concentrations of BCF, suggesting that cellulose fibrils did not promote the formation of a
427 more organised structure even in the presence of amylose, during our storage conditions.
428

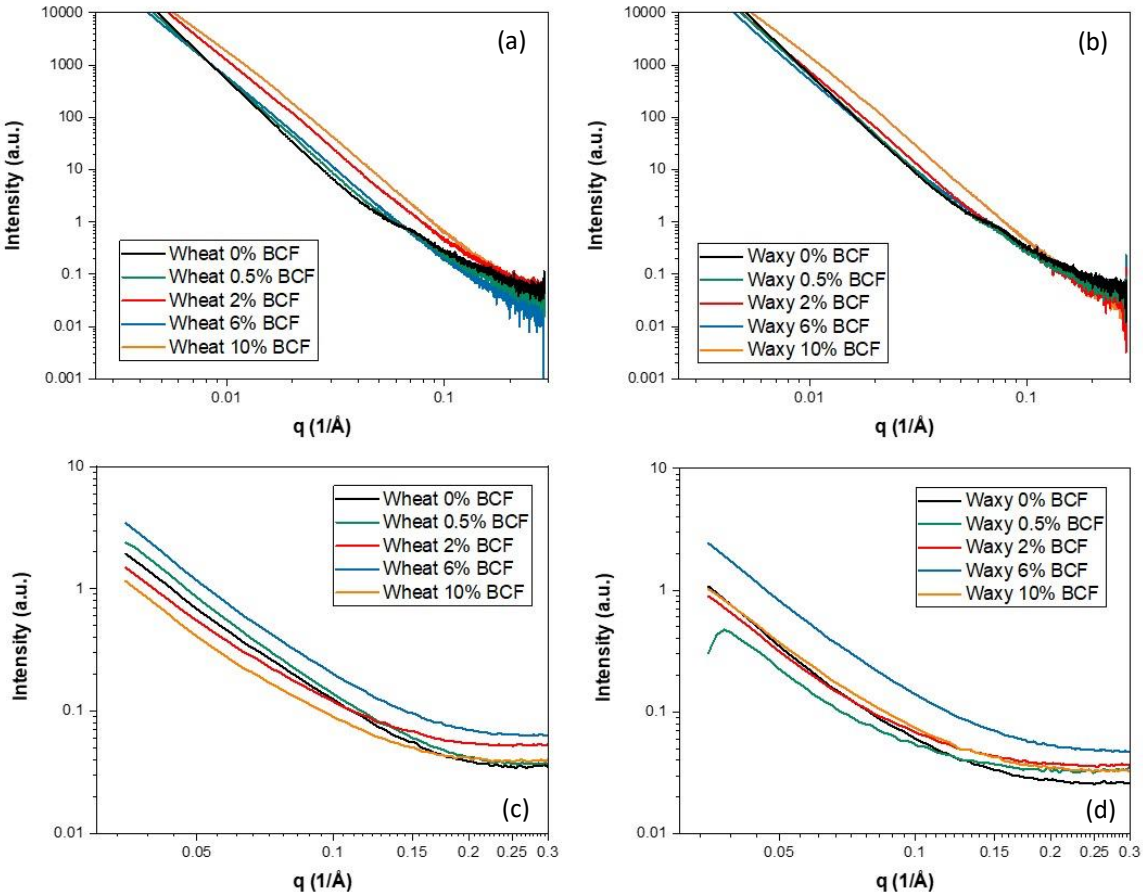

Figure 4. SAXS patterns of starch-bacterial cellulose fibrils (BCF) blends: (a) native wheat-BCF (synchrotron), and (b) native waxy-BCF. Samples processed by RVA and freeze-dried: (c) wheat-BCF, and (d) waxy-BCF.

Figure 5 (e and f) shows the WAXS patterns of native waxy-maize and wheat starches compared with samples processed by RVA and subsequently freeze dried. The diffraction peaks of the processed samples are significantly lower in intensity and broader than that of the native starches which indicates a loss in crystallinity, and supporting that processing created defects in the regular packing and disruption of amylose and amylopectin helices. This also confirms that processed samples, as expected from observation of the SAXS region, have not regained the same level or order of native starches, and therefore they present a more disordered structure after processing.

442 The effect of BCF on the structure of BCF-starch samples can be deducted by comparison of
443 Figure 5 (a and b) and Figure 5 (c and d). The two graphs on Figure 5 (c, d) show WAXS patterns
444 of freeze dried BCF-starch samples processed by RVA and stored 24h at 4° C, while the former
445 two graphs show freeze dried physical mixtures of native starches and BCF (Figure 5, a and b)
446 collected by synchrotron radiation. The WAXS peaks at around 1.0, 1.2, 1.4 and 1.6 $Å^{-1}$, in both
447 processed starch samples at different concentration of BCF are of cellulose origin, as shown in
448 the WAXS pattern of pure BCF (Figure SF-3, Supplementary File). As might be expected their
449 intensity increased with the increase in concentration of BCF. On the other hand, there are no
450 significant differences in intensity in the characteristic peaks of waxy/wheat starches as a
451 function of BCF concentration. Thus, BCF did not seem to promote a more organised structure
452 of starch compared to the starch samples at 0% BCF. Interestingly, WAXS pattern of processed
453 wheat and waxy-maize starch did not show marked differences among each other (in a similar
454 way observed also in native starch samples), also supporting the fact that amylose should be
455 only partly self-associated in our samples. It is worth noticing that the tested solid samples had
456 considerably different size distributions but they were all measured in capillaries of the same,
457 fixed volume. This is the reason for the significant differences in absolute peak intensities among
458 samples.
459 Nano and sub-nano characterisation by SAXS/WAXS of partly retrograded BCF-starch blends
460 showed good correlation with the rheology data (Figures 1, 2 and 3), particularly with the
461 behaviour of the loss factor. Both techniques suggest that BCF did not promote the regain of
462 organized structure of blend during storage. Therefore, the observed increase in G' (Figure 1 and
463 2) could be explained by the contribution of the cellulose itself to the whole stiffness of the partly
464 self-associated material, presumably acting as a filler, rather than promoting a more complex and
465 organised structure. However, at this point it is also necessary to consider the potential role of
466 water. Recently it has been reported that completely gelatinised starch blended with BCF is
467 organised in structural domains rich in either starch or cellulose (Díaz-Calderón et al., 2018). In

such phase separated microstructures cellulose would tend to hold water in its own structural domain, and therefore water available to the starch in the starch phase could be insufficient for amylose self-association, which under these conditions may occur at a much higher temperature. It could be considered as a possible explanation of the behaviour showed by our results, and worth to be investigated in future research.

Figure 6 (a and b) shows a comparison between the microstructure of wheat starch and waxy-maize starch in the absence of BCF and with BCF via SEM imaging. It seems there is no significant difference between the two structures. Indeed, in both starchy samples a honeycomb-like structure is observed, which is typical of freeze-dried starch samples and where void spaces were originally occupied by water (Figure 6). This porous structure was not modified by the presence of bacterial cellulose, and a similar structure is observed among BCF-starches samples showing a non-homogenous distribution of cellulose fibrils in the matrix and the presence of cellulose fibrils embebbed into the starchy walls (Figure 7). Previous studies have reported the non-homogeneous distribution of BCF in gelatin based films, and also in starchy blends (Díaz-Calderón et al., 2018; Quero et al., 2015). Hence, BCF did not significantly affect the microstructure of the two starch samples during the storage and partial retrogradation. For a complete comparison, images of physical mixtures prior to RVA processing of starch and BCF as well as pure BCF fibrils are shown in the Supplementary Information (Figures SF-4 and SF-5).

486

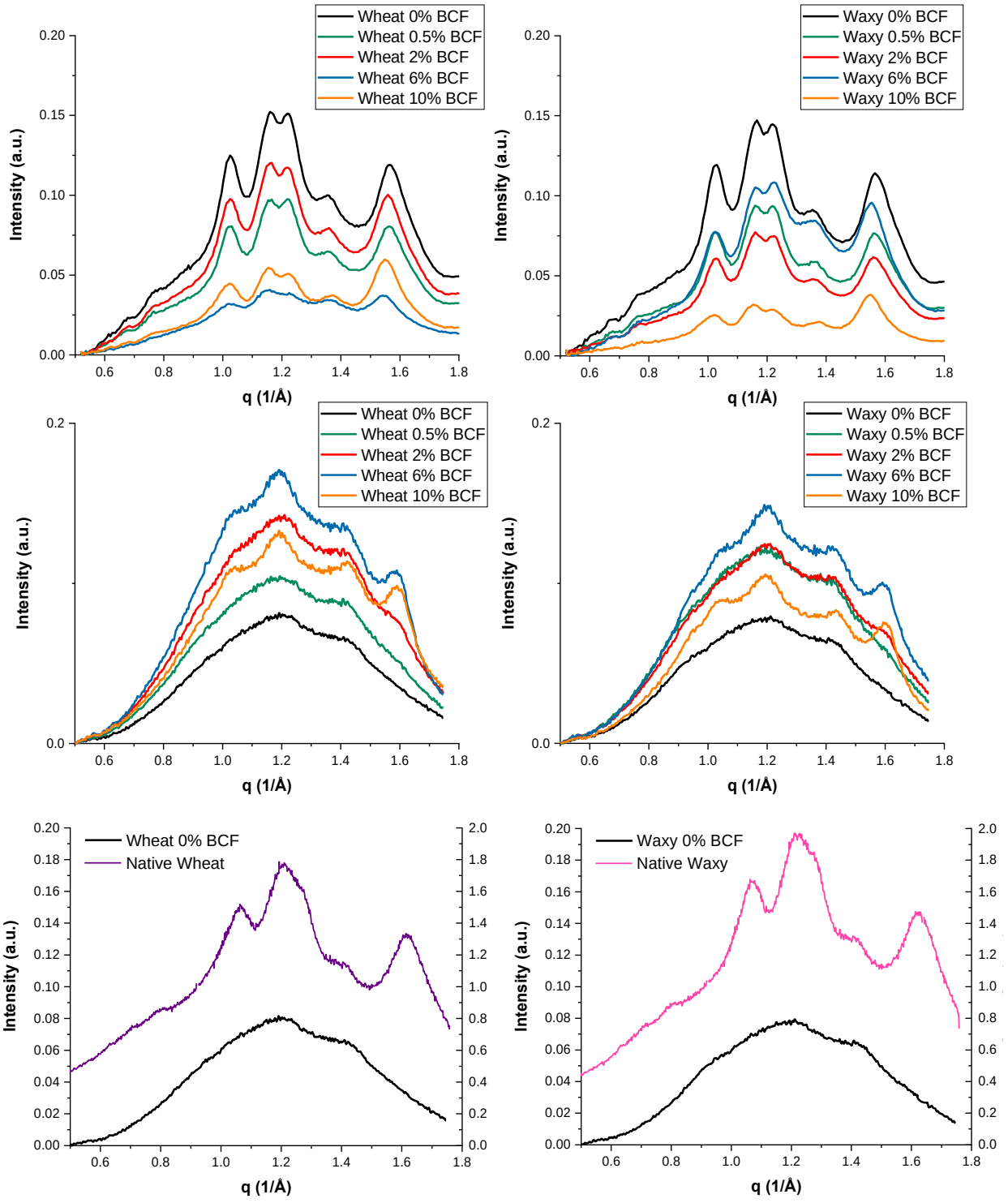
Wheat 0% BCF
Wheat 0.5% BCF
Wheat 2% BCF
Wheat 6% BCF
Wheat 10% BCF
Waxy 0% BCF
Waxy 0.5% BCF
Waxy 2% BCF
Waxy 6% BCF
Waxy 10% BCF
Native Wheat
Native Waxy
Intensity (a.u.)
q (1/Å)

487

488

Figure 5. Synchrotron WAXS pattern of starch-bacterial cellulose fibrils (BCF) blends: (a) native wheat-BCF, (b) native waxy-maize-BCF. Benchtop WAXS pattern of processed by RVA and freeze-dried: (c) wheat-BCF, (d) waxy-maize-BCF. Comparison of benchtop WAXS pattern of native and freeze-dried processed: (e) wheat and (f) waxy-maize starch.

(a)

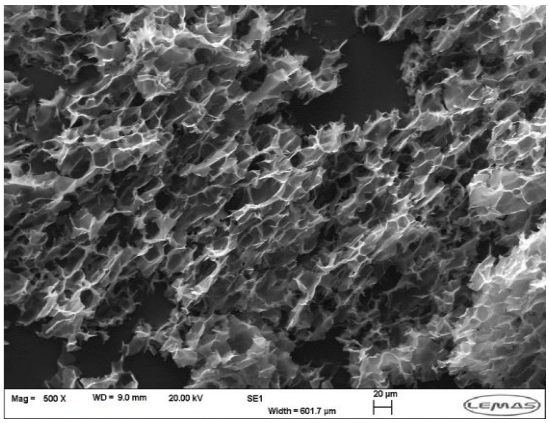

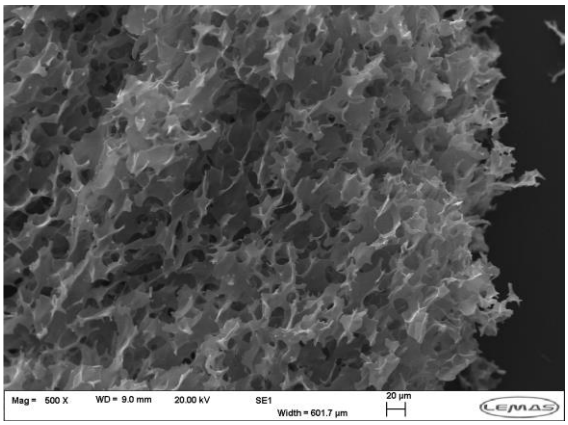

(b)

(c)

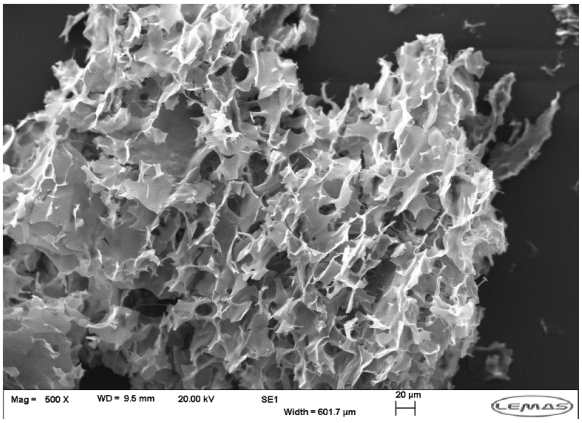

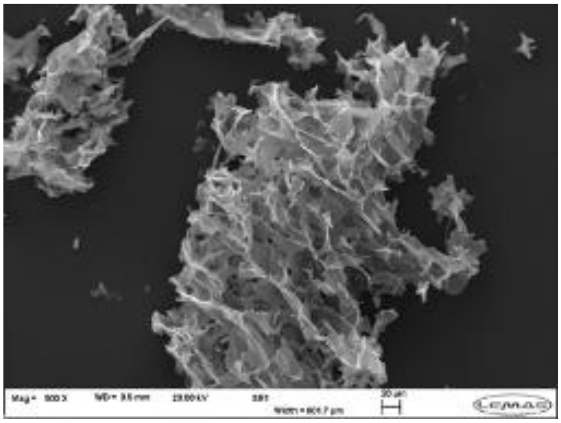

(d)

Figure 6: SEM images of starch- bacterial cellulose fibrils (BCF) blends processed by RVA, stored at 4°C for 24 hrs and freeze-dried used for SAXS/WAXS analysis: (a) wheat 0%BCF, (b) waxy-maize 0%BCF, (c) wheat 10% BCF, and (d) waxy 10% BCF.

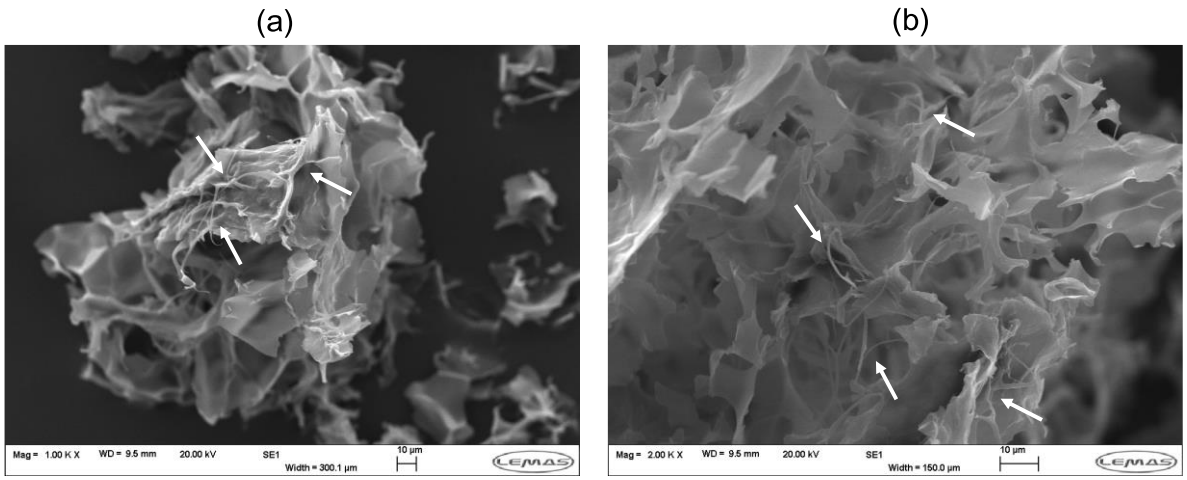

Figure 7: SEM images of starch- bacterial cellulose fibrils (BCF) blends processed by RVA, stored at 4°C for 24 hrs and freeze-dried used for SAXS/WAXS analysis: (a) wheat starch and 2%BCF; (b) wheat starch and 6%BCF. White arrows indicate the presence of BCF

3.4. Gel strength in partly retrograded starch-BCF blends

The results of gel strength measurements carried out on partly retrograded starch-BCF blends after storage at 4°C for 24 h are presented in Figure 8 (a, b). The gel strength values observed in our samples was strongly dependent on the starch type. Indeed, pure wheat starch showed a higher gel strength value (~160g) compared to waxy-maize (~90g). This difference could be related to the partial self-association of amylose in wheat starch, contributing to a stiffer network within the matrix (Wang et al., 2015). When BCF was present with each starch, a complex mechanical response was observed. In wheat starch, BCF at concentration of 0.5%, 2% and 6% produced a significant decrease in gel strength. However, at 10%, there was an increase in gel strength, but significantly lower ($p<0.05$) than the control sample. In waxy-maize starch the addition of BCF also had a complex effect on the gel strength, showing the lowest value at

517 concentration of 0.5% BCF but increasing the gel strength to higher values than the control in
518 samples containing BCF in concentrations of 6% (w/w) or more.
519

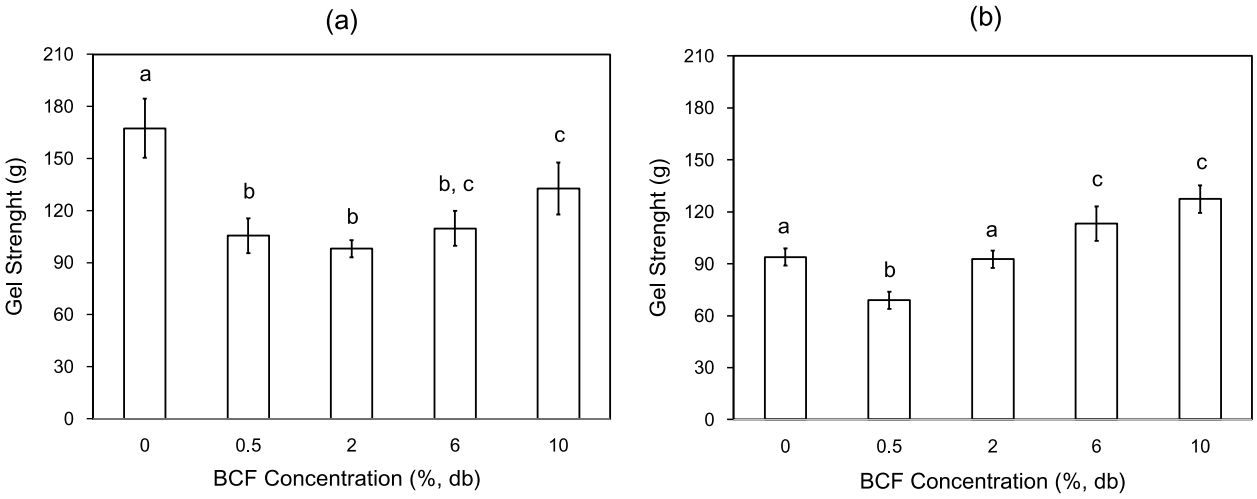

520
521 **Figure 8.** Gel strength in partly retrograded starch- bacterial cellulose fibrils (BCF) samples
522 (24h, 4° C): (a) wheat, (b) waxy-maize. Different lowercase letters show significant differences
523 among samples (p-value < 0.05).
524

525 In the literature, the gel strength has been explained by the ability of soft materials to recover
526 stable helical structures during the storage after the complete thermal unfolding of native
527 structures (Wang et al, 2015). In starch based systems, the time-dependent process of
528 reassociation, under certain environmental conditions of temperature and moisture, can be
529 followed by changes in the gel strength (Lionetto et al., 2005; Ottenhof, Hill & Farhat, 2005). Thus,
530 gel strength has been considered as a way to follow the retrogradation of starch (Wang et al.,
531 2015; Xia et al., 2014), where amylose and amylopectin recover the helical structure lost during
532 the gelatinisation. The lower values of gel strength depicted in Figure 8 agree with rheology data
533 and with nano/sub-nano characterisation. Thus, the weakening effect of BCF on starch blends
534 (Figure 3) and the inability of starch to recover a semi-crystalline organisation (Figure 4 and
535 Figure 5) are well reflected by the gel strength data, which suggest a partial reassociation of

starch during storage. The fact that polymer fibrils restrict the reassociation of starch has been previously reported by the literature. For instance, Xia et al. (2014) reported from a mechanical testing that cellulose, hemicellulose and lignin had a retarding effect on the retrogradation of rice starch (reflecting an anti-staling effect), which was reflected by lower hardness in retrograded gels in presence of these cellulose derivatives which was also correlated with a decrease in crystallinity assessed by X-ray diffraction. Similar findings were reported by Zhang et al. (2018a) in corn starch and pectin blends, where pectin restricted the rearrangement of starch producing a reduction in gel strength and crystallinity (assessed by X-Ray diffraction) in 7 and 14 days retrograded gels. Most recently, Ma et al. (2019) reported a retardation of retrogradation in corn starch by effect of konjac glucomannan (KGM) with different molecular weights, reflected by a significant decrease in retrogradation enthalpy and corresponding decrease in crystallinity. This behavior was explained by the high-water absorption ability of KGM and its steric exclusion associated with the leached amylose by intense hydrogen bonding. All of the above indicate that when starch is gelatinised in the presence of another polymer, the leaching of amylose from the granule is affected due to thermodynamic phase separation effects (Appelqvist & Debet, 1997). Our results suggest that mechanical response of the retrograded starch-BCF gels could be governed by the aggregation of cellulose fibrils taking place at higher BCF inclusion levels (Chen et al., 2020) overriding the effect of self-association of amylose. For instance, it is noticeable that there were not significant differences in terms of gel strength among wheat and waxy-maize starch gels containing BCF in concentrations of 2% (w/w) or higher, as it was also previously seen in the viscoelastic characterization (Figures 1 and 2, Table SF-2 in Supplementary File). Indeed, recorded values of gel strength showed good correlation with values of G' reported in the frequency sweep test. However, the gel strength of pure wheat starch gels and those containing 0.5% BCF were significantly higher than those one observed in waxy-maize starch with the same BCF content, presumably because amylose partly self-associated is addressing the mechanical response in starchy gels with very low BCF concentration. This should be the reason why in

562 Figure 8, the highest gel strength was reached by wheat starch gel without BCF, although the
563 role of time, moisture content, temperature and even differences in structure attributed to the
564 sample preparation for gel strength assessment cannot be neglected. Likewise, the absence of
565 interaction between starch and BCF due to the cellulose structure could also be considered to
566 explain the weakness of starchy gels in presence of BCF. The complexity of the bacterial cellulose
567 structure would support the role played by volume fraction of BCF in defining the mechanical and
568 rheological effect on starchy based systems, as discussed previously in Section 3.1 and also
569 depicted by SEM images, and that the leaching of amylose from starch granules can delay the
570 effectiveness of cellulose in creating such structures.
571
572 **4. Conclusions**
573 The role of BCF on the self-association during early stages of starch retrogradation showed that
574 BCF produced a significant increase in final viscosity and setback viscosity in both starches, with
575 the relative increase, when compared with the control, being greater in the waxy maize sample.
576 However, the viscoelastic characterisation of starch-BCF blends showed that samples containing
577 BCF were less organised (because of the increase in loss factor values), despite of the higher
578 values of G' in frequency sweep test observed in samples with higher BCF concentration (6% and
579 10% w/v), reflecting a system whose rheological properties are dominated by cellulose fibrils
580 within a cellulose-rich phase. This rheological behaviour showed good agreement with the
581 characterisation by SAXS/WAXS, which showed that our samples did not fully recover an ordered
582 starch structure. SEM images of these samples showed that BCF did not modify the
583 microstructure of partly retrograded samples. Mechanical response of partly retrograded samples
584 showed complex behaviour, reflecting the partly self-association of amylose at low values of BCF,
585 and the contribution of cellulose to the mechanical response at higher values of BCF, in
586 agreement with rheological and nano/sub-nano characterisation. Therefore, our results showed
587 that BCF did not promote the self-association of amylose at least during early stages of

retrogradation. Further studies are necessary to elucidate the role of bacterial cellulose in terms of holding water and its volume fraction in the bulk system, along with the role of available water to allow the amylose self-association. These findings can be used as an input for the rational design of starch-BCF composites as advanced materials with tunable physical properties and tailored structures for specific industrial applications.

5. Acknowledgements

Authors would like to thank the financial support received from FONDECYT Grant Nº1191375, REDES Grant Nº180089 and Fondo de Apoyo a la Investigación FAI UANDES. Experimental support in the assessment of mechanical properties carried out by Belén Astorga and Daniela Medina from the School of Nutrition and Dietetics of Universidad de los Andes, and quite valuable scientific discussions given by Dra. Laura Iturriaga (Universidad Nacional de Santiago del Estero, Argentina) are warmly acknowledged. We thank Diamond Light Source and beamline I22 for the award of beam time (proposal SM22659-1) and Professor Nick Terrill and Dr. Tim Snow for support. The Bragg Centre for Materials Research at the University of Leeds is also acknowledged. We would also like to dedicate this paper to Emeritus Professor John R. Mitchell who inspired the work, was co-author on our first publication in this series and built bridges between the UK and Chile.

6. References

Appelqvist, I. A. M. & Debet, M. R. M. (1997) Starch - biopolymer interactions—a review. *Food Reviews International*, 13(2), 163-224, https://doi.org/10.1080/87559129709541105

Balet, S., Guelpa, A., Fox, G., & Manley, M. (2019). Rapid Visco Analyser (RVA) as a tool for measuring starch-related physiochemical properties in cereals: a review. *Food Analytical*

Methods, *12*(10), 2344–2360. https://doi.org/10.1007/s12161-019-01581-w

Basiak, E., Lenart, A., & Debeaufort, F. (2017). Effect of starch type on the physico-chemical properties of edible films. *International Journal of Biological Macromolecules*, *98*, 348–356. https://doi.org/10.1016/j.ijbiomac.2017.01.122

Belitz, H. D., Grosch, W., & Schieberle, P. (2009). *Food Chemistry* (4th Editio). Springer Verlag. https://doi.org/10.1007/978-3-540-69934-7

BeMiller, J. N., & Huber, K. H. (2008). Carbohydrates. In S. Damodaran, K. L. Parkin, & O. R. Fennema (Eds.), *Fenemma's Food Chemistry* (Fourth Edi, pp. 83–154). CRC Press.

Benito-González, I., López-Rubio, A., & Martínez-Sanz, M. (2019). High-performance starch biocomposites with celullose from waste biomass: Film properties and retrogradation behaviour. *Carbohydrate Polymers*, *216*, 180–188. https://doi.org/10.1016/j.carbpol.2019.04.030

Chang, W.-S., & Chen, H.-H. (2016). Physical properties of bacterial cellulose composites for wound dressings. *Food Hydrocolloids*, *53*, 75–83. https://doi.org/10.1016/j.foodhyd.2014.12.009

Chen, D., Fang, F., Federici, E., Campanella, O., & Griffith Jones, O. (2020). Rheology, microstructure and phase behavior of potato starch-protein fibril mixed gel. *Carbohydrate Polymers*, *239*, 116247.

Cui, S., Li, M., Zhang, S., Liu, J., Sun, Q., & Xiong, L. (2018). Physicochemical properties of maize and sweet potato starches in the presence of cellulose nanocrystals. *Food Hydrocolloids*, *77*, 220–227. https://doi.org/10.1016/j.foodhyd.2017.09.037

Díaz-Calderón, P., MacNaughtan, B., Hill, S., Foster, T., Enrione, J., & Mitchell, J. (2018). Changes in gelatinisation and pasting properties of various starches (wheat, maize and waxy maize) by the addition of bacterial cellulose fibrils. *Food Hydrocolloids*, *80*, 274–280. https://doi.org/10.1016/j.foodhyd.2018.02.023

Doutch, J., & Gilbert, E. P. (2013). Characterisation of large scale structures in starch granules via small-angle neutron and X-ray scattering. *Carbohydrate Polymers*, *91*(1), 444–451. https://doi.org/10.1016/j.carbpol.2012.08.002

640 Fadel, G., Luiz, C., Rita, M., Aurélio, M., Novak, C., Fernandes, C., Souza, D., Amado, A., Alves, R.,
641 & Freitas, D. (2017). Bacterial cellulose in biomedical applications : A review. *International Journal*
642 *of Biological Macromolecules*, *104*, 97–106. https://doi.org/10.1016/j.ijbiomac.2017.05.171
643 Fazeli, M., Keley, M., & Biazar, E. (2018). Preparation and characterization of starch-based
644 composite films reinforced by cellulose nanofibers. *International Journal of Biological*
645 *Macromolecules*, *116*, 272–280. https://doi.org/10.1016/j.ijbiomac.2018.04.186
646 Filik, J., Ashton, A. W., Chang, P. C. Y., Chater, P. A., Day, S. J., Drakopoulos, M., Gerring, M. W.,
647 Hart, M. L., Magdysyuk, O. V., Michalik, S., Smith, A., Tang, C. C., Terrill, N. J., Wharmby, M. T., &
648 Wilhelm, H. (2017). Processing two-dimensional X-ray diffraction and small-angle scattering data
649 in DAWN 2. *Journal of Applied Crystallography*, *50*(3), 959–966.
650 https://doi.org/10.1107/S1600576717004708
651 He, F., Li, X. L., Luo, H., Liang, H., Wan, Y. Z., & Huang, Y. (2009). Mechanical, moisture
652 absorption, and biodegradation behaviours of bacterial cellulose fibre-reinforced starch
653 biocomposites. *Composites Science and Technology*, *69*(7–8), 1212–1217.
654 https://doi.org/10.1016/j.compscitech.2009.02.024
655 Hornung, P. S., Avila, S., Masisi, K., Malunga, L. N., Lazzarotto, M., Schnitzler, E., Ribani, R. H., &
656 Beta, T. (2018). Green development of biodegradable films based on native yam (Dioscoreaceae)
657 starch mixtures. *Starch*, *70(5-6)*,*1700234*. https://doi.org/10.1002/star.201700234
658 Ikeda, S., & Nishinari, K. (2001). " Weak gel"-type rheological properties of aqueous dispersions
659 of nonaggregated k-carrageenan helices. *Journal of Agricultural and Food Chemistry*, *49*(9),
660 4436–4441.
661 Ilyas, R. A., Sapuan, S. M., Ishak, M. R., & Zainudin, E. S. (2018). Development and
662 characterization of sugar palm nanocrystalline cellulose reinforced sugar palm starch
663 bionanocomposites. *Carbohydrate Polymers*, *202*, 186–202.
664 https://doi.org/10.1016/j.carbpol.2018.09.002
665 Juhász, R., & Salgó, A. (2008). Pasting behavior of amylose, amylopectin and their mixtures as

666 determined by RVA curves and first derivatives. *Starch/Staerke*, *60*(2), 70–78.
667 https://doi.org/10.1002/star.200700634
668 Kim, H., & Bemiller, J. N. (2012). Effects of hydrocolloids on the pasting and paste properties of
669 commercial pea starch. *Carbohydrate Polymers*, *88*(4), 1164–1171.
670 https://doi.org/10.1016/j.carbpol.2012.01.060
671 Lee, K. Y., Buldum, G., Mantalaris, A., & Bismarck, A. (2014). More than meets the eye in bacterial
672 cellulose: Biosynthesis, bioprocessing, and applications in advanced fiber composites.
673 *Macromolecular Bioscience*, *14*(1), 10–32. https://doi.org/10.1002/mabi.201300298
674 Leite, T. D., Nicoleti, J. F., Lúcia, A., Penna, B., Maria, C., & Franco, L. (2012). Effect of addition
675 of different hydrocolloids on pasting , thermal , and rheological properties of cassava starch.
676 *Ciencia e Tecnologia de Alimentos, 32*(3), 579–587.
677 Li, M., Xie, F., Hasjim, J., Witt, T., Halley, P. J., & Gilbert, R. G. (2015). Establishing whether the
678 structural feature controlling the mechanical properties of starch films is molecular or crystalline.
679 *Carbohydrate Polymers*, *117*, 262–270. https://doi.org/10.1016/j.carbpol.2014.09.036
680 Lionetto, F., Maffezzoli, A., Ottenhof, M. A., Farhat, I. A., & Mitchell, J. R. (2005). The
681 retrogradation of concentrated wheat starch systems. *Starch/Staerke*, *57*(1), 16–24.
682 https://doi.org/10.1002/star.200400298
683 Luchese, L., Spada, J. C., & Tessaro, I. C. (2018). Impact of the starch source on the
684 physicochemical properties and biodegradability of different starch-based films. *Journal of*
685 *Applied Polymer Journal, 46564*, 1–11. https://doi.org/10.1002/app.46564
686 Ma, S., Zhu, P., Wang, M., Wang, F., & Wang, N. (2019). Effect of konjac glucomannan with
687 different molecular weights on physicochemical properties of corn starch. *Food Hydrocolloids*,
688 *96*, 663–670. https://doi.org/10.1016/j.foodhyd.2019.06.014
689 Mezger, T. G. (2019). *Applied Rheology* (6th Editio). Anton Paar GmbH.
690 Miao, C., & Hamad, W. Y. (2013). Cellulose reinforced polymer composites and nanocomposites:
691 a critical review. *Cellulose*, *20*(5), 2221–2262. https://doi.org/10.1007/s10570-013-0007-3

692 Müller, C. M. O., Laurindo, J. B., & Yamashita, F. (2009). Effect of cellulose fibers addition on the
693 mechanical properties and water vapor barrier of starch-based films. *Food Hydrocolloids*, *23*(5),
694 1328–1333. https://doi.org/10.1016/j.foodhyd.2008.09.002
695 Ottenhof, M. A., Hill, S. E., & Farhat, I. A. (2005). Comparative study of the retrogradation of
696 intermediate water content waxy maize, wheat, and potato starches. *Journal of Agricultural and*
697 *Food Chemistry*, *53*(3), 631–638. https://doi.org/10.1021/jf048705y
698 Paximada, P., Tsouko, E., Kopsahelis, N., Koutinas, A. A., & Mandala, I. (2016). Bacterial cellulose
699 as stabilizer of o/w emulsions. *Food Hydrocolloids*, *53*, 225–232.
700 https://doi.org/10.1016/j.foodhyd.2014.12.003
701 Qiu, S., Yadav, M. P., Liu, Y., Chen, H., Tatsumi, E., & Yin, L. (2014). Effects of corn fiber gum with
702 different molecular weights on the gelatinization behaviors of corn and wheat starch. *Food*
703 *Hydrocolloids*, *53*, 180–186. https://doi.org/10.1016/j.foodhyd.2015.01.034
704 Quero, F., Coveney, A., Lewandowska, A. E., Richardson, R. M., Díaz-Calderón, P., Lee, K. Y.,
705 Eichhorn, S. J., Alam, M. A., & Enrione, J. (2015). Stress transfer quantification in gelatin-matrix
706 natural composites with tunable optical properties. *Biomacromolecules*, *16*(6), 1784–1793.
707 https://doi.org/10.1021/acs.biomac.5b00345
708 Rajwade, J. M., Paknikar, K. M., & Kumbhar, J. V. (2015). Applications of bacterial cellulose and
709 its composites in biomedicine. *Applied Microbiology and Biotechnology*, *99*(6), 2491–2511.
710 https://doi.org/10.1007/s00253-015-6426-3
711 Romdhane, I. H., Price, P. E., Miller, C. A., Benson, P. T., & Wang, S. (2001). Drying of glassy
712 polymer films. *Industrial & Engineering Chemical Research 40*, 3065–3075.
713 Sadashiv, V., Ravindra, P., Dyawanapelly, S., Deshpande, A., Jain, R., & Dandekar, P. (2018).
714 Bioactive materials starch based nano fibrous scaffolds for wound healing applications. *Bioactive*
715 *Materials*, *3*(3), 255–266. https://doi.org/10.1016/j.bioactmat.2017.11.006
716 Shah, N., Ul-Islam, M., Khattak, W. A., & Park, J. K. (2013). Overview of bacterial cellulose
717 composites: A multipurpose advanced material. *Carbohydrate Polymers*, *98*(2), 1585–1598.

718 https://doi.org/10.1016/j.carbpol.2013.08.018
719 Shi, Z., Zhang, Y., Phillips, G. O., & Yang, G. (2014). Utilization of bacterial cellulose in food. *Food*
720 *Hydrocolloids*, *35*, 539–545. https://doi.org/10.1016/j.foodhyd.2013.07.012
721 Sun, J., Sheng, X. Z., Xu, F. H., Chen, J., & Chen, Y. M. T. (2016). Effects of cellulose derivative
722 hydrocolloids on pasting , viscoelastic , and morphological characteristics of rice starch gel.
723 *Journal of Texture Studies*, *48(3)*, 241–248. https://doi.org/10.1111/jtxs.12233
724 Ullah, H., Santos, H. A., & Khan, T. (2016). Applications of bacterial cellulose in food , cosmetics
725 and drug delivery. *Cellulose*, *23*, 2291–2314. https://doi.org/10.1007/s10570-016-0986-y
726 Valencia, G. A., Zare, E. N., Makvandi, P., & Gutiérrez, T. J. (2019). Self-assembled carbohydrate
727 polymers for food applications: a review. *Comprehensive Reviews in Food Science and Food*
728 *Safety*, *18*(6), 2009–2024. https://doi.org/10.1111/1541-4337.12499
729 Velasquez, D., Pavon-djavid, G., Chaunier, L., Meddahi-pellé, A., & Lourdin, D. (2015). Effect of
730 crystallinity and plasticizer on mechanical properties and tissue integration of starch-based
731 materials from two botanical origins. *Carbohydrate Polymers*, *124*, 180–187.
732 https://doi.org/10.1016/j.carbpol.2015.02.006
733 Wang, S., Li, C., Copeland, L., Niu, Q., & Wang, S. (2015). Starch retrogradation: a comprehensive
734 review. *Comprehensive Reviews in Food Science and Food Safety*, *14*(5), 568–585.
735 https://doi.org/10.1111/1541-4337.12143
736 Xia, W., Fu, G., Liu, C., Zhong, Y., Zhong, J., Luo, S., & Liu, W. (2014). Effects of cellulose, lignin
737 and hemicellulose on the retrogradation of rice starch. *Food Science and Technology Research*,
738 *20*(2), 375–383. https://doi.org/10.3136/fstr.20.375
739 Yang, J., Lv, X., Chen, S., Li, Z., Feng, C., Wang, H., & Xu, Y. (2014). In situ fabrication of a
740 microporous bacterial cellulose/potato starch composite scaffold with enhanced cell
741 compatibility. *Cellulose*, *21*(3), 1823–1835. https://doi.org/10.1007/s10570-014-0220-8
742 Yildiz, Ö., Yurt, B., Ba, A., Said, Ö., Tahsin, M., Karaman, S., & Da, O. (2013). Pasting properties,
743 texture profile and stress–relaxation behavior of wheat starch/dietary fiber systems. *Food*

744 *Research International, 53*, 278–290. https://doi.org/10.1016/j.foodres.2013.04.018
745 Zang, S., Zhang, R., Chen, H., Lu, Y., Zhou, J., Chang, X., Qiu, G., Wu, Z., & Yang, G. (2015).
746 Investigation on artificial blood vessels prepared from bacterial cellulose. *Materials Science and*
747 *Engineering C*, *46*, 111–117. https://doi.org/10.1016/j.msec.2014.10.023
748 Zhang, B., Bai, B., Pan, Y., Li, X., Cheng, J., & Chen, H. (2018). Effects of pectin with different
749 molecular weight on gelatinization behavior, textural properties, retrogradation and in vitro
750 digestibility of corn starch. *Food Chemistry*, *264*, 58–63.
751 https://doi.org/10.1016/j.foodchem.2018.05.011
752